A MARGINALISED PARTICLE FILTER FOR BEARINGS-ONLY TRACKING

Mark R. Morelande

Melbourne Systems Laboratory
The University of Melbourne
Parkville VIC 3010
email: mrmore@unimelb.edu.au

ABSTRACT

A marginalised particle filter (PF) for bearings-only tracking in modified polar coordinates (MPC) is developed. Using an Euler approximation to the dynamical equation it is shown that the range can be marginalised out so that only the three remaining elements of the state vector need to be sampled in the PF. The marginalised PF in MPC is shown to significantly outperform existing PFs for BOT in a numerical example.

Index Terms— Particle filters; bearings-only tracking; nonlinear filters.

1. INTRODUCTION

In bearings-only tracking (BOT) the aim is to estimate the trajectory of a moving object using noisy direction measurements taken by a moving sensor. This is an important problem in several applications, such as passive sonar and radar tracking where directional information is obtained by sensing signals emitted from an object [1].

BOT is usually approached in a Bayesian framework in which the aim is to compute the posterior density. Given the posterior density, the minimum mean square error estimator, the posterior mean, can be computed. Since the posterior density is not available in closed-form for BOT the challenge is to find an accurate yet computationally efficient approximation. The most common method is to approximate the posterior by a Gaussian [2, 3, 4, 5]. Gaussian approximations to the posterior are computationally efficient, since they represent the posterior with relatively few parameters, and can be surprisingly accurate in many cases. However, a Gaussian density can only approximate a non-Gaussian posterior density with a limited degree of accuracy.

Particle filters (PFs) offer the possibility of arbitrarily accurate approximation of the posterior, albeit with increased computational expense [6]. A PF is a recursive Monte Carlo method which represents the posterior by weighted random samples, usually drawn from an importance density. In order to be a viable solution in practice, PFs must be carefully designed. A review of techniques which can be used to improve PF performance can be found in [6].

In this paper we consider the use of a particular PF improvement strategy referred to as marginalisation, or Rao-Blackwellisation. Marginalisation replaces Monte Carlo approximation with analytical computation wherever possible. This can be done, for example, if the dynamical and measurement models are linear and Gaussian for some elements of the state conditional on the remaining elements [7]. This situation arises in BOT with the velocity elements of the state vector forming the "linear/Gaussian" part of the state vector so that only the position elements need to be sampled. However, a marginalised PF exploiting this structure provided no discernible improvements in performance when applied to various BOT problems in [8].

A somewhat different approach to marginalisation for BOT is pursued here. The first element of our approach is to represent the object kinematics in modified polar coordinates (MPC). MPC were proposed in [2] to handle the fact that the range of an object moving with constant velocity is not observable until the sensor platform manoeuvres. In MPC the unobservable range is decoupled from the remaining elements of the state vector. The second element of our approach is to use an Euler approximation [9] to the dynamical equation rather than the exact equation. Once this is done it can be shown that, conditional on the other elements of the state vector, inference on the range can be performed analytically. As a result only three of the four elements of the state vector need to be sampled in the PF.

Most PFs for BOT represent the state in Cartesian coordinates [10, 11, 12] although log polar coordinates, which are closely related to MPC, were used in [13]. Marginalisation for BOT in Cartesian coordinates was used in [8], albeit with no appreciable benefit. The novelty of this paper is to apply marginalisation to BOT in MPC. This will be seen to provide a major improvement in performance for the numerical example considered here.

The paper is organised as follows. The dynamical model for MPC is given in Section 2 for both Cartesian coordinates and MPC. The marginalised PF is developed in Section 3 and its performance is compared with several PFs in Section 4.

2. MODEL

We begin by specifying the dynamical model in Cartesian coordinates and then show how a dynamical model for modified polar coordinates (MPC) can be obtained using the Euler approximation.

2.1. Cartesian coordinates

For $t \in \mathbb{R}$, the object kinematics relative to the sensor are collected into the vector $\mathbf{z}(t) = [x(t), y(t), \dot{x}(t), \dot{y}(t)]'$ where $(x(t), y(t))$ is target position relative to the sensor at time t and the dot notation indicates differentiation with respect to time. The motion of an object which moves with a random walk in velocity can be modelled by the stochastic differential equation (SDE)

$$\dot{\mathbf{z}}(t) = \mathbf{A}\mathbf{z}(t) + \mathbf{B}(\mathbf{w}(t) - \mathbf{a}(t)), \tag{1}$$

where $\mathbf{w}(t)$ is a white Gaussian noise process with power spectral density matrix $q\mathbf{I}_2$, $\mathbf{a}(t)$ is the sensor acceleration and

$$\mathbf{A} = \begin{bmatrix} 0 & 1 \\ 0 & 0 \end{bmatrix} \otimes \mathbf{I}_2, \tag{2}$$

$$\mathbf{B} = \begin{bmatrix} 0 \\ 1 \end{bmatrix} \otimes \mathbf{I}_2. \tag{3}$$

In (2) and (3), $\mathbf{I}_d$ is the $d \times d$ identity matrix and $\otimes$ is the Kronecker product.

Measurements are acquired with sampling period T. The object state at the time of the kth measurement is denoted as $\mathbf{z}_k = \mathbf{z}(kT)$. The evolution of the target state over a sampling period is found by discretising (1) to give

$$\mathbf{z}_k = \mathbf{F}\mathbf{z}_{k-1} - \mathbf{u}_k + \mathbf{w}_k \tag{4}$$

where $\mathbf{w}_k$ are independent zero-mean Gaussian random variables with covariance matrix $\mathbf{Q}$, $\mathbf{u}_k$ is the input due to sensor movement and

$$\mathbf{F} = \begin{bmatrix} 1 & T \\ 0 & 1 \end{bmatrix} \otimes \mathbf{I}_2, \tag{5}$$

$$\mathbf{Q} = q \begin{bmatrix} T^3/3 & T^2/2 \\ T^2/2 & T \end{bmatrix} \otimes \mathbf{I}_2. \tag{6}$$

2.2. Modified polar coordinates

The state vector in MPC at time $t \in \mathbb{R}$ is denoted as $\mathbf{x}(t) = [\beta(t), r(t), \dot{\beta}(t), \dot{\rho}(t)]'$ where $\beta(t)$ is the direction of the object, $r(t)$ is the range and $\dot{\rho}(t) = \dot{r}(t)/r(t)$. Let $\mathbf{x}_k = \mathbf{x}(kT)$. Note that the MPC formulation used here differs from [2] since we use range rather than inverse range.

The discrete-time evolution of the state vector in MPC can be obtained using (4) and the transformation $\mathbf{e} : \mathbb{R}^4 \to \mathbb{R}^4$ from MPC to relative Cartesian coordinates. This gives

$$\mathbf{x}_k = \mathbf{e}^{-1}(\mathbf{F}\,\mathbf{e}(\mathbf{x}_{k-1}) - \mathbf{u}_k + \mathbf{w}_k) \tag{7}$$

Instead of using the exact discrete-time dynamical equation (7), we return to the SDE governing object motion in MPC and construct an Euler approximation [9]. Although using an approximation when the exact dynamics are available may seem nonsensical, the use of an Euler approximation for the dynamics is instrumental in the development of an efficient marginalised PF.

The SDE in MPC corresponding to (1) can be found as

$$\dot{\mathbf{x}}(t) = \mathbf{c}(\mathbf{x}(t)) + \mathbf{D}(\mathbf{x}(t))(\mathbf{w}(t) - \mathbf{a}(t)) \tag{8}$$

where, for $\mathbf{x} = [\beta, r, \dot{\beta}, \dot{\rho}]$,

$$\mathbf{c}(\mathbf{x}) = \begin{bmatrix} \dot{\beta} \\ r\dot{\rho} \\ -2\dot{\rho}\dot{\beta} \\ \dot{\beta}^2 - \dot{\rho}^2 \end{bmatrix}, \tag{9}$$

$$\mathbf{D}(\mathbf{x}) = 1/r \begin{bmatrix} \mathbf{0}_2 \\ -\sin(\beta) & \cos(\beta) \\ \cos(\beta) & \sin(\beta) \end{bmatrix}. \tag{10}$$

with $\mathbf{0}_d$ a $d \times d$ matrix of zeros. The Euler approximation of (7) is

$$\mathbf{x}_k \approx \mathbf{f}(\mathbf{x}_{k-1}) + \mathbf{D}(\mathbf{x}_{k-1})(\mathbf{v}_k - T\mathbf{a}_{k-1}) \tag{11}$$

where $\mathbf{f}(\mathbf{x}) = \mathbf{x} + T\mathbf{c}(\mathbf{x})$, $\mathbf{v}_k$ are independent zero-mean Gaussian random variables with covariance matrix $qT\mathbf{I}_2$ and $\mathbf{a}_{k-1} = \mathbf{a}((k-1)T)$. The Euler approximation (11) becomes exact as $T \to 0$.

The measurement ϕ_k taken at time kT satisfies

$$\phi_k = \beta_k + e_k \tag{12}$$

where $e_1, e_2, \ldots$ are independent zero-mean Gaussian random variables with variance κ. The process noise $\{\mathbf{v}_k\}$ and measurement noise $\{e_k\}$ are independent.

3. MARGINALISED PARTICLE FILTER

In this section the marginalised PF is developed by first establishing a preliminary result and then showing how this result can be used to avoid sampling the range. Some details involved in the implementation of the filter are also discussed.

3.1. Preliminary result

Consider the following density parameterised by $\boldsymbol{\theta} = [\nu, \tau, \omega]$, $\nu \in \mathbb{N}$, $\tau \in \mathbb{R}$, $\omega > 0$:

$$\mathsf{M}(r; \boldsymbol{\theta}) = r^\nu \exp(-\omega(r-\tau)^2)/C(\boldsymbol{\theta}),\ r > 0, \tag{13}$$

where

$$C(\boldsymbol{\theta}) = \int_0^\infty r^\nu \exp(-\omega(r-\tau)^2)\,\mathrm{d}r \tag{14}$$

Let $\mathsf{N}(\cdot; \boldsymbol{\mu}, \boldsymbol{\Sigma})$ denote the Gaussian density with mean $\boldsymbol{\mu}$ and covariance matrix $\boldsymbol{\Sigma}$. We then have the following.

Lemma 1. *For* $\mathbf{p} \in \mathbb{R}^m$,

$$\mathsf{N}(\mathbf{p}; \boldsymbol{\mu}/r, \boldsymbol{\Sigma}/r^2)\mathsf{M}(r; \boldsymbol{\theta}) = f(\mathbf{p}; \boldsymbol{\mu}, \boldsymbol{\Sigma}, \boldsymbol{\theta})\mathsf{M}(r; \tilde{\boldsymbol{\theta}}) \tag{15}$$

where $\tilde{\boldsymbol{\theta}} = [\tilde{\nu}, \tilde{\tau}, \tilde{\omega}]'$ *with* $\tilde{\nu} = \nu + m$ *and*

$$\tilde{\tau} = \tau + \mathbf{g}(\boldsymbol{\mu} - \mathbf{p}\tau) \tag{16}$$

$$\tilde{\omega} = \omega/(1 - \mathbf{g}\mathbf{p}) \tag{17}$$

$$f(\mathbf{p}; \boldsymbol{\mu}, \boldsymbol{\Sigma}, \boldsymbol{\theta}) = \frac{C(\tilde{\boldsymbol{\theta}})}{\tau^m C(\boldsymbol{\theta})} \sqrt{\frac{\tilde{\omega}}{\omega}} \mathsf{N}(\mathbf{p}; \boldsymbol{\mu}/\tau, \mathbf{S}(\mathbf{p})/\tau^2) \tag{18}$$

where $\mathbf{g} = \mathbf{p}'\mathbf{S}(\mathbf{p})^{-1}/(2\omega)$ *and* $\mathbf{S}(\mathbf{p}) = \mathbf{p}\mathbf{p}'/(2\omega) + \boldsymbol{\Sigma}$.

Proof. The product can be written as

$$\begin{aligned} &\mathsf{N}(\mathbf{p}; \boldsymbol{\mu}/r, \boldsymbol{\Sigma}/r^2)\mathsf{M}(r; \boldsymbol{\theta}) \\ &= \frac{r^{\nu+m}}{C(\boldsymbol{\theta})} \sqrt{\frac{\pi}{\omega}}\, \mathsf{N}(\boldsymbol{\mu}; \mathbf{p}r, \boldsymbol{\Sigma})\mathsf{N}(r; \tau, 1/(2\omega)) \qquad (19) \\ &= \frac{r^{\nu+m}}{C(\boldsymbol{\theta})} \sqrt{\frac{\pi}{\omega}} \mathsf{N}(\boldsymbol{\mu}; \mathbf{p}\tau, \mathbf{S}(\mathbf{p}))\mathsf{N}(r; \tilde{\tau}, 1/(2\tilde{\omega})) \qquad (20) \end{aligned}$$

where the Gaussian product lemma [14] has been used to obtain (20). The result (15) follows directly. □

3.2. Development of the marginalised PF

We now show how Lemma 1 can be used to construct a marginalised PF for BOT using the Euler approximation (11). Let $\boldsymbol{\xi}_k = [\beta_k, \dot{\beta}_k, \dot{\rho}_k]'$. Assume the availability at time $(k-1)T$ of a posterior density approximation consisting of samples $\boldsymbol{\xi}_{k-1}^1, \ldots, \boldsymbol{\xi}_{k-1}^n$ with associated weights $w_{k-1}^1, \ldots, w_{k-1}^n$ along with the parameters $\boldsymbol{\theta}_{k-1}^1, \ldots, \boldsymbol{\theta}_{k-1}^n$ of the posterior density of the range r_{k-1} conditional on each sample. The posterior density $\pi_{k-1}(\cdot)$ can then be approximated as

$$\pi_{k-1}(\mathbf{x}_{k-1}) \approx \sum_{i=1}^n w_{k-1}^i \delta(\boldsymbol{\xi}_{k-1} - \boldsymbol{\xi}_{k-1}^i)\mathsf{M}(r_{k-1}; \boldsymbol{\theta}_{k-1}^i) \tag{21}$$

It will be shown that a posterior density approximation of the same form can be obtained at time kT. Before continuing it is convenient to define the partition $\boldsymbol{\xi}_k = [\beta_k, \boldsymbol{\zeta}_k']'$, $\boldsymbol{\zeta}_k = [\dot{\beta}_k, \dot{\rho}_k]'$ where, according to the Euler approximation (11), the evolution of $\boldsymbol{\zeta}_k$ satisfies

$$\boldsymbol{\zeta}_k | \mathbf{x}_{k-1} \sim \mathsf{N}(\cdot; \mathbf{h}(\boldsymbol{\zeta}_{k-1}) + \mathbf{s}_k(\beta_{k-1})/r_{k-1}, \mathbf{P}/r_{k-1}^2) \tag{22}$$

where $\sim$ means "is distributed as" and

$$\mathbf{h}(\boldsymbol{\zeta}) = \begin{bmatrix} \dot{\beta} - 2T\dot{\rho}\dot{\beta} \\ \dot{\rho} + T(\dot{\beta}^2 - \dot{\rho}^2) \end{bmatrix}, \tag{23}$$

$$\mathbf{s}_k(\beta) = T \begin{bmatrix} \sin(\beta) & -\cos(\beta) \\ -\cos(\beta) & -\sin(\beta) \end{bmatrix} \mathbf{a}_{k-1}, \tag{24}$$

$$\mathbf{P} = qT\mathbf{I}_2 \tag{25}$$

The prior density can be found, using (11) and (22), as

$$\begin{aligned} \varpi_k(\mathbf{x}_k) = &\int \delta(\beta_k - (\beta + T\dot{\beta}))\, \delta(r_k - r(1 + T\dot{\rho})) \\ &\times \mathsf{N}(\boldsymbol{\zeta}_k; \mathbf{h}(\boldsymbol{\zeta}) + \mathbf{s}_k(\beta)/r, \mathbf{P}/r^2)\pi_{k-1}(\mathbf{x})\, \mathrm{d}\mathbf{x} \end{aligned} \tag{26}$$

Substituting the PF approximation of $\pi_{k-1}(\cdot)$ into (26) gives

$$\begin{aligned} \varpi_k(\mathbf{x}_k) \approx &\sum_{i=1}^{n} w_{k-1}^i \delta(\beta_k - \tilde{\beta}_k^i) \int \mathsf{N}(\boldsymbol{\zeta}_k; \mathbf{h}_k^i + \mathbf{s}_k^i/r, \mathbf{P}/r^2) \\ &\times \mathsf{M}(r; \boldsymbol{\theta}_{k-1}^i)\delta(r_k - r(1 + T\dot{\rho}_{k-1}^i))\, \mathrm{d}r \end{aligned} \tag{27}$$

where $\tilde{\beta}_k^i = \beta_{k-1}^i + T\dot{\beta}_{k-1}^i$, $\mathbf{h}_k^i = \mathbf{h}(\boldsymbol{\zeta}_{k-1}^i)$ and $\mathbf{s}_k^i = \mathbf{s}_k(\beta_{k-1}^i)$. Using Lemma 1 gives

$$\begin{aligned} \varpi_k(\mathbf{x}_k) \approx &\sum_{i=1}^{n} w_{k-1}^i \delta(\beta_k - \tilde{\beta}_k^i) f(\boldsymbol{\zeta}_k - \mathbf{h}_k^i; \mathbf{s}_k^i, \mathbf{P}, \boldsymbol{\theta}_{k-1}^i) \\ &\times \int \delta(r_k - r(1 + T\dot{\rho}_{k-1}^i))\mathsf{M}(r; \hat{\boldsymbol{\theta}}_{k-1}^i(\boldsymbol{\zeta}_k))\, \mathrm{d}r \end{aligned} \tag{28}$$

where $\hat{\boldsymbol{\theta}}_{k-1}^i(\boldsymbol{\zeta}) = [\hat{\nu}_{k-1}^i, \hat{\tau}_{k-1}^i(\boldsymbol{\zeta}), \hat{\omega}_{k-1}^i(\boldsymbol{\zeta})]'$ with $\hat{\nu}_{k-1}^i = \nu_{k-1}^i + 2$ and

$$\hat{\tau}_{k-1}^i(\boldsymbol{\zeta}) = \tau_{k-1}^i + \mathbf{g}_k^i(\boldsymbol{\zeta})[\mathbf{s}_{k-1}^i - (\boldsymbol{\zeta} - \mathbf{h}_{k-1}^i)\tau_{k-1}^i] \tag{29}$$

$$\hat{\omega}_{k-1}^i(\boldsymbol{\zeta}) = \omega_k^i/[1 - \mathbf{g}_k^i(\boldsymbol{\zeta})(\boldsymbol{\zeta} - \mathbf{h}_{k-1}^i)] \tag{30}$$

with $\mathbf{g}_k^i(\boldsymbol{\zeta}) = (\boldsymbol{\zeta} - \mathbf{h}_{k-1}^i)\mathbf{S}_k^i(\boldsymbol{\zeta})^{-1}$ and $\mathbf{S}_k^i(\boldsymbol{\zeta}) = (\boldsymbol{\zeta} - \mathbf{h}_{k-1}^i)(\boldsymbol{\zeta} - \mathbf{h}_{k-1}^i)' + 2\omega_{k-1}^i\mathbf{P}$. Evaluating the remaining integral gives

$$\begin{aligned} \varpi_k(\mathbf{x}_k) \approx &\sum_{i=1}^{n} w_{k-1}^i \delta(\beta_k - \tilde{\beta}_k^i) f(\boldsymbol{\zeta}_k - \mathbf{h}_k^i; \mathbf{s}_k^i, \mathbf{P}, \boldsymbol{\theta}_{k-1}^i) \\ &\times \mathsf{M}(r_k; \tilde{\boldsymbol{\theta}}_k^i(\boldsymbol{\zeta}_k)) \end{aligned} \tag{31}$$

where $\tilde{\boldsymbol{\theta}}_k^i(\boldsymbol{\zeta}) = [\tilde{\nu}_k^i, \tilde{\tau}_k^i(\boldsymbol{\zeta}), \tilde{\omega}_k^i(\boldsymbol{\zeta})]'$ with $\tilde{\nu}_k^i = \hat{\nu}_{k-1}^i$ and

$$\tilde{\tau}_k^i(\boldsymbol{\zeta}) = (1 + T\dot{\rho}_{k-1}^i)\hat{\tau}_{k-1}^i(\boldsymbol{\zeta}) \tag{32}$$

$$\tilde{\omega}_k^i(\boldsymbol{\zeta}) = \hat{\omega}_{k-1}^i/(1 + T\dot{\rho}_{k-1}^i)^2 \tag{33}$$

The posterior density at time kT can be found, using Bayes' rule, as

$$\pi_k(\mathbf{x}_k) \propto \mathsf{N}(\phi_k; \beta_k, \kappa)\varpi_k(\mathbf{x}_k) \tag{34}$$

where we have used the measurement equation (12). After substituting the prior density approximation (31) into (34) it can be seen that the posterior density decomposes into a product of the terms:

$$\begin{aligned} \pi_k(\boldsymbol{\xi}_k) \propto &\mathsf{N}(\phi_k; \beta_k, \kappa) \sum_{i=1}^{n} w_{k-1}^i \delta(\beta_k - \tilde{\beta}_k^i) \\ &\times f(\boldsymbol{\zeta}_k - \mathbf{h}_k^i; \mathbf{s}_k^i, \mathbf{P}, \boldsymbol{\theta}_{k-1}^i) \end{aligned} \tag{35}$$

$$\pi_k(r_k|\boldsymbol{\xi}_k) = \mathsf{M}(r_k; \tilde{\boldsymbol{\theta}}_k^i(\boldsymbol{\zeta}_k)) \tag{36}$$

An approximation to the posterior can now be obtained by sampling from (35) and evaluating (36) for each sample of $\boldsymbol{\xi}_k$.

To construct a Monte Carlo approximation of $\pi_k(\boldsymbol{\xi}_k)$ we first reverse the marginalisation over the sample index in the mixture (35), as in [11]. This permits the important resampling step [10] to enter into the sampling procedure in a natural manner. We have

$$\begin{aligned} \pi_k(\boldsymbol{\xi}_k, i) &\propto w_{k-1}^i \mathsf{N}(\phi_k; \beta_k, \kappa)\delta(\beta_k - \tilde{\beta}_k^i) \\ &\quad \times f(\boldsymbol{\zeta}_k - \mathbf{h}_k^i; \mathbf{s}_k^i, \mathbf{P}, \boldsymbol{\theta}_{k-1}^i) \qquad (37) \\ &= \delta(\beta_k - \tilde{\beta}_k^i)\pi_k(\boldsymbol{\zeta}_k, i) \qquad (38) \end{aligned}$$

where

$$\pi_k(\boldsymbol{\zeta}_k, i) \propto w_{k-1}^i \mathsf{N}(\phi_k; \tilde{\beta}_k^i, \kappa) f(\boldsymbol{\zeta}_k - \mathbf{h}_k^i; \mathbf{s}_k^i, \mathbf{P}, \boldsymbol{\theta}_{k-1}^i) \tag{39}$$

It is clear that only $\boldsymbol{\zeta}_k$ and the auxiliary variable i can be sampled since, given i, we have $\beta_k = \tilde{\beta}_k^i$. A sample of size n can be drawn directly from (39) as follows. For $a = 1, \ldots, n$, set $i^a = j$ with probability proportional to $w_{k-1}^j \mathsf{N}(\phi_k; \tilde{\beta}_k^j, \kappa)$ and then draw $\boldsymbol{\zeta}_k^a \sim f(\cdot - \mathbf{h}_k^{i^a}; \mathbf{s}_k^{i^a}, \mathbf{P}, \boldsymbol{\theta}_{k-1}^{i^a})$. Since samples are drawn directly from (39) the sample weights are uniform, i.e., $w_k^i = 1/n$. Finally, we set $\beta_k^a = \tilde{\beta}_k^{i^a}$ and compute the parameters $\boldsymbol{\theta}_k^a = \tilde{\boldsymbol{\theta}}_k^{i^a}(\boldsymbol{\zeta}_k^a)$.

3.3. Implementation details

For simplicity the marginalised PF for BOT has been developed with the Euler approximation applied over the whole sampling period of duration T. This is likely to result in poor performance for large T. At the expense of additional computations, it is straightforward to divide the sampling period into m intervals and apply the Euler approximation over intervals of duration T/m. This results in Algorithm 1. The quantity $\mathbf{s}_k(\beta; t)$ appearing in lines 5 and 17 is computed as shown in (24) with $\mathbf{a}_{k-1}$ replaced by $\mathbf{a}((k-1)T + t)$.

The algorithm calls for samples to be drawn from the non-standard density $f(\cdot)$ given in (18). To do this we note that

$$f(\boldsymbol{\zeta} - \mathbf{h}; \mathbf{s}, \mathbf{P}, \boldsymbol{\theta}) = \int \mathsf{N}(\boldsymbol{\zeta}; \mathbf{h} + \mathbf{s}/r, \mathbf{P}/r^2)\mathsf{M}(r; \boldsymbol{\theta})\, \mathrm{d}r \tag{40}$$

Therefore, $\boldsymbol{\zeta}$ can be sampled by drawing $r \sim \mathsf{M}(\cdot; \boldsymbol{\theta})$ and then drawing $\boldsymbol{\zeta} \sim \mathsf{N}(\cdot; \mathbf{h} + \mathbf{s}/r, \mathbf{P}/r^2)$. The problem is then to draw from the non-standard distribution $\mathsf{M}(\cdot; \boldsymbol{\theta})$. This can be done by rejection sampling [15] using a truncated Gaussian density over $(0, \infty)$ with mean $r^*(\boldsymbol{\theta})$ and variance $1/(2\omega)$ where $r^*(\boldsymbol{\theta})$ is the location of the peak of $\mathsf{M}(\cdot; \boldsymbol{\theta})$. This is given by, for $\tau > 0$,

$$r^*(\boldsymbol{\theta}) = \tau\big(1 + \sqrt{1 + 2\nu/(\tau^2\omega)}\big)/2 \tag{41}$$

Although its derivation is not given here for the sake of brevity, the bounding constant is close to unity in most cases indicating that samples from the proposal are usually accepted.

Clearly the marginalised PF will not converge to the true posterior as the sample size $n \to \infty$ due to errors introduced by the Euler approximation. It may be conjectured that as $m \to \infty$, so that the Euler approximation becomes exact, the marginalised PF will converge to the true posterior as $n \to \infty$ but this remains to be proved.

4. NUMERICAL EXAMPLE

The numerical example used to analyse the performance of the marginalised PF is as follows. An object with an initial range of 5 km and bearing 10° moves at a constant speed of 4 knots with a

Algorithm 1: Marginalised particle filter for BOT

for $i = 1, \ldots, n$ **do** set $\boldsymbol{\xi}_k^i(0) = \boldsymbol{\xi}_{k-1}^i$ and $\boldsymbol{\theta}_k^i(0) = \boldsymbol{\theta}_{k-1}^i$;
for $j = 1, \ldots, m-1$ **do**
  for $i = 1, \ldots, n$ **do**
    compute $\beta_k^i(j) = \beta_k^i(j-1) + T\dot{\beta}_k^i(j-1)/m$;
    compute $\mathbf{h}_k^i(j) = \mathbf{h}(\boldsymbol{\zeta}_k^i(j-1))$ and $\mathbf{s}_k^i(j) = \mathbf{s}_k(\tilde{\beta}_k^i(j-1); (j-1)T/m)$;
    draw $\boldsymbol{\zeta}_k^i(j) \sim f(\cdot - \mathbf{h}_k^i(j); \mathbf{s}_k^i(j), \mathbf{P}, \boldsymbol{\theta}_k^i(j-1))$;
    compute $\boldsymbol{\theta}_k^i(j) = \tilde{\boldsymbol{\theta}}_k^i(\boldsymbol{\zeta}_k^i(j))$;
  end
end
for $i = 1, \ldots, n$ **do**
  set $\tilde{\beta}_k^i = \beta_k^i(m-1) + T\dot{\beta}_k^i(m-1)/m$;
  compute $\tilde{\psi}^i = \mathsf{N}(\phi_k; \tilde{\beta}_k^i, \kappa)$
end
for $i = 1, \ldots, n$ **do** compute $\psi^i = \tilde{\psi}^i / \sum_{j=1}^n \tilde{\psi}^j$;
for $i = 1, \ldots, n$ **do**
  set $a = j$ with probability ψ^j;
  compute $\mathbf{h}_k^i = \mathbf{h}(\boldsymbol{\zeta}_k^a(m-1))$ and $\mathbf{s}_k^i = \mathbf{s}_k(\beta_k^a(m-1); (m-1)T/m)$;
  draw $\boldsymbol{\zeta}_k^i \sim f(\cdot - \mathbf{h}_k^i; \mathbf{s}_k^i, \mathbf{P}, \boldsymbol{\theta}_k^a(m-1))$;
  set $\beta_k^i = \tilde{\beta}_k^a$;
  compute $\boldsymbol{\theta}_k^i(j) = \tilde{\boldsymbol{\theta}}_k^a(\boldsymbol{\zeta}_k^i)$;
end

heading -130°. The object is observed by a sensor which produces measurements every $T = 60$ seconds. The sensor moves at a constant speed of 5 knots with initial heading -45°. Between the 13th and 17th sampling instants the sensor executes a turn at a constant rate of $0.5^\circ/\text{s}$. The sensor then continues along the new heading until the surveillance period ends after 30 sampling periods. The measurement noise standard deviation is set to 1°. This example, which has previously been used in [12, 16], is illustrated in Fig. 1.

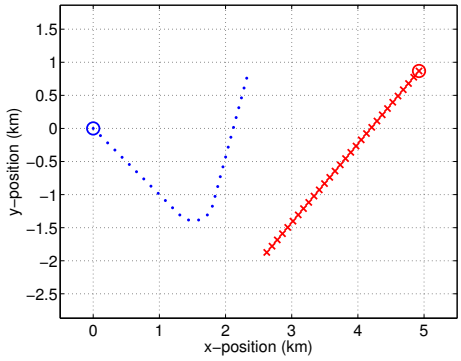

Fig. 1. Simulation scenario: The sensor trajectory is indicated by the blue dots and the object trajectory is indicated by the red crosses. Circles are placed at the trajectory starting points.

The proposed algorithm, referred to as the marginalised PF in MPC (MPF-MPC), is compared to several existing PFs. A bootstrap filter (BF), as proposed in [10], is considered in both Cartesian coordinates and MPC. These filters are referred to as the BF-C and BF-MPC, respectively. The BF-MPC is implemented with the exact dynamical equation (7) rather than the Euler approximation. We also consider the marginalised PF in Cartesian coordinates, referred to as the MPF-C, as proposed in [8]. The MPF-MPC employs the Euler approximation over $m = 4$ intervals per sampling period. Although no process noise exists in the object motion, the filters assume a small amount of process noise. In particular, the process noise covariance matrix is as shown in (6) with $q = 10^{-8}$.

The filters are initialised with the aid of the first measurement, as described in [16]. The initial bearing and heading are determined from the measurement. The initial bearing is from the distribution $\mathsf{N}(\phi_1, \kappa)$. It is assumed the object is headed toward the sensor, although with a large degree of uncertainty, so that the initial heading is distributed as $\mathsf{N}(\phi_1 + \pi, (45\pi/180)^2)$. Prior information on the object range and speed is assumed to be available so that the initial range, in km, is distributed as $\mathsf{N}(10, 9)$ and the initial speed, in knots, has the distribution $\mathsf{N}(16, 36)$. The considerable amount of uncertainty in the prior, coupled with the initial non-observability of the range, make this a difficult filtering problem.

The filters are implemented with sample sizes between $n = 10^3$ and $n = 10^5$. For each sample size, the RMS position error is computed by averaging over 1000 realisations. The RMS position errors averaged over the last 10 sampling instants of the surveillance period are plotted against sample size in Fig. 2. The best performance is clearly achieved by the MPF-MPC. It obtains the same accuracy as BF-C, BF-MPC and MPF-C, which perform similarly, with less than $1/10$ the sample size. The similarity in the performances of the BF-C and MPF-C is in accordance with results given in [8]. The saving in sample size achieved by the MPF-MPC is offset somewhat by a greater computational expense per particle: roughly four times that of the BF-MPC and seven times that of the BF-C and MPF-C in our implementation.

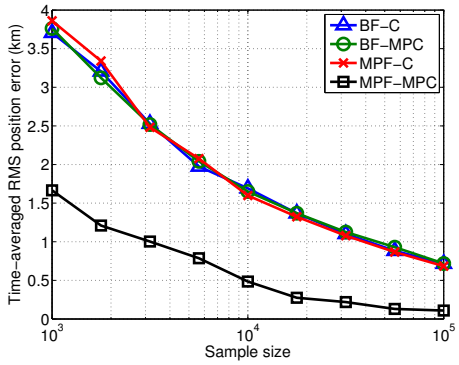

Fig. 2. Time-averaged RMS position error plotted against sample size for the BF-C, BF-MPC, MPF-C and MPF-MPC.

5. CONCLUSIONS

A marginalised particle filter for bearings-only tracking has been developed. The proposed filter exploits the structure of the Euler approximation to the dynamical equation of the state in modified polar coordinates. Significant improvement over existing particle filters was obtained in a numerical example.

Future work includes an exploration of how the accuracy of the Euler approximation affects performance and the extension to tracking in three dimensions.

6. REFERENCES

[1] A. Farina, "Target tracking with bearings-only measurements," *Signal Processing*, vol. 78, pp. 61–78, 1999.

[2] V.J. Aidala and S.E. Hammel, "Utilization of modified polar coordinates for bearings-only tracking," *IEEE Transactions on Automatic Control*, vol. 28, no. 3, pp. 283–294, 1983.

[3] J.M.C. Clark, R.B. Vinter, and M.M. Yaqoob, "Shifted Rayleigh filter: A new algorithm for bearings-only tracking," *IEEE Transaction on Aerospace and Electronic Systems*, vol. 43, no. 4, pp. 1373–1384, 2007.

[4] M.R. Morelande, L. Svensson, J. Hagmar, and M. Jirstrand, "Optimal posterior density approximation for bearings-only tracking," in *Proceedings of IEEE International Conference on Acoustics, Speech and Signal Processing*, Kyoto, Japan, 2012.

[5] N. Peach, "Bearings-only tracking using a set of range-parameterised extended Kalman filters," *IEE Proceedings-Control Theory Applications*, vol. 142, no. 1, pp. 73–80, 1995.

[6] O. Cappé, S.J. Godsill, and E. Moulines, "An overview of existing methods and recent advances in sequential Monte Carlo," *Proceedings of the IEEE*, vol. 95, no. 5, pp. 899–924, 2007.

[7] T. Schon, F. Gustafsson, and P-J. Nordlund, "Marginalized particle filters for mixed linear/nonlinear state-space models," *IEEE Transactions on Signal Processing*, vol. 53, no. 7, pp. 2279–2289, 2005.

[8] R. Karlsson and F. Gustafsson, "Recursive Bayesian estimation: bearings-only applications," *IEE Proceedings on Radar Sonar and Navigation*, vol. 152, no. 5, pp. 305–313, 2005.

[9] P.E. Kloeden and E. Platen, *Numerical Solution of Stochastic Differential Equations*, Springer Verlag, 1992.

[10] N.J. Gordon, D.J. Salmond, and A.F.M. Smith, "Novel approach to nonlinear/non-Gaussian Bayesian state estimation," *IEE Proceedings Part F*, vol. 140, no. 2, pp. 107–113, 1993.

[11] M.K. Pitt and N. Shephard, "Filtering via simulation: auxiliary particle filters," *Journal of the American Statistical Association*, vol. 94, pp. 590–599, 1999.

[12] B. Ristic, M.S. Arulampalam, and N.J. Gordon, *Beyond the Kalman Filter: Particle Filters for Tracking Applications*, Artech House, 2004.

[13] T. Brehard and J-P. Le Cadre, "Hierarchical particle filter for bearings only tracking," *IEEE Transactions on Aerospace and Electronic Systems*, vol. 43, no. 4, pp. 1567–1585, 2007.

[14] Y.C. Ho and R.C.K. Lee, "A Bayesian approach to problems in stochastic estimation and control," *IEEE Transactions on Automatic Control*, vol. 9, pp. 333–339, 1964.

[15] R.Y. Rubinstein and D.P. Kroese, *Simulation and the Monte Carlo Method*, Wiley, Hoboken, NJ, 2008.

[16] B. La Scala and M.R. Morelande, "An analysis of the single-sensor bearings-only tracking problem," in *Proceedings of the International Conference on Information Fusion*, Colgone, Germany, 2008.